analytical chemistry

pubs.acs.org/ac

Article

Development and Analytical Validation of a One-Step Five-Plex RT-ddPCR Assay for the Quantification of SARS-CoV-2 Transcripts in Clinical Samples

Areti Strati,* Martha Zavridou, Dimitrios Paraskevis, Gkikas Magiorkinis, Spyros Sapounas, Pagona Lagiou, Nikolaos S. Thomaidis, and Evi S. Lianidou*

Cite This: https://doi.org/10.1021/acs.analchem.2c00868

Read Online

ACCESS | Metrics & More | Article Recommendations | Supporting Information

ABSTRACT: Highly sensitive methodologies for SARS-CoV-2 detection are essential for the control of COVID-19 pandemic. We developed and analytically validated a highly sensitive and specific five-plex one-step RT-ddPCR assay for SARS-CoV-2. We first designed in-silico novel primers and probes for the simultaneous absolute quantification of three different regions of the nucleoprotein (*N*) gene of SARS-CoV-2 (N1, N2, N3), a synthetic RNA as an external control (RNA-EC), and Beta-2-Microglobulin (*B2M*) as an endogenous RNA internal control (RNA-IC). The developed assay was analytically validated using synthetic DNA and RNA calibrator standards and then was applied to 100 clinical specimens previously analyzed with a commercially available CE-IVD RT-qPCR assay. The analytical validation of the developed assay resulted in very good performance characteristics in terms of analytical sensitivity, linearity, analytical specificity, and reproducibility and recovery rates even at very low viral concentrations. The simultaneous absolute quantification of the RNA-EC and RNA-IC provides the necessary metrics for quality control assessment. Direct comparison of the developed one-step five-plex RT-ddPCR assay with a CE-IVD RT-qPCR kit revealed a very high concordance and a higher sensitivity [concordance: 99/100 (99.0%, Spearman's correlation coefficient: −0.850, $p < 0.001$)]. The developed assay is highly sensitive, specific, and reproducible and has a broad linear dynamic range, providing absolute quantification of SARS-COV-2 transcripts. The inclusion of two RNA quality controls, an external and an internal, is highly important for standardization of SARS-COV-2 molecular testing in clinical and wastewater samples.

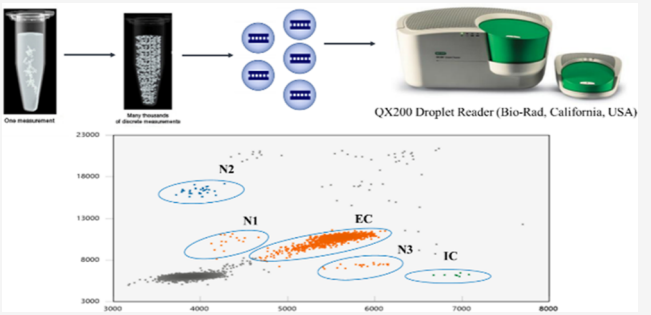

INTRODUCTION

WHO has reported more than 423 million confirmed cases of severe acute respiratory syndrome coronavirus 2 (SARS-CoV-2) cases and 5.8 million coronavirus disease 2019 (COVID-19) related deaths, by the mid of February 2022. The early characterization of the causative agent of COVID-19 allowed for the development of molecular tests for the diagnosis of SARS-CoV-2 infections.[1] Currently, there are two different types of tests: the viral and the antibody tests. The former category includes the nucleic acid amplification tests (NAATs) and the antigen tests, used to detect active infection with SARS-CoV-2.[2−4] The antibody tests are used to detect past infection with SARS-CoV-2,[5,6] while they are not recommended to test for immunity after vaccination or natural infection.[7]

NAATs are highly sensitive and specific and are considered as the gold standard methods for SARS-CoV-2 diagnosis. They target one or more genes (i.e., *ORF1*, *N*, and *S* genes) and detect current infection.[8] Due to the prolonged virus shedding in different organs, in some instances, viral RNA can be detected for a long time after viral infection without evidence that the virus can replicate or infect other individuals.[9,10] On the other hand, due to early appearance of viral RNA, NAATs have higher sensitivity than antigen tests for the diagnosis of asymptomatic or presymptomatic infection.[8] The quantification cycle (C_q) value has been used as a proxy of viral concentration that can be used to predict transmissibility and severity of disease and to differentiate prolonged viral shedding from active infection. Several factors including the quality of specimen, patient factors, as well as the assay characteristics can affect the C_q value of the RT-qPCR result.[11]

Droplet digital PCR (ddPCR) represents an accurate molecular tool for the absolute quantification of target molecules at very low concentrations.[12] The main principle

Received: February 22, 2022
Accepted: August 1, 2022

of ddPCR is the partitioning of reaction mixture in an extremely high number of droplets and the detection of fluorescence at the end of PCR amplification. According to Poisson distribution, the fraction of positive droplets determines the number of target copies per unit without the need for calibration curves.[13] Moreover, amplification inhibitors are divided into different sub-reactions, thus increasing resistance of ddPCR reaction to inhibitors and providing high stability.[12] Another important feature of ddPCR assays is that sensitivity is not affected by the background of nucleic acid extracts.[14]

Up to now, many different RT-ddPCR assays have been developed for the quantification of SARS-CoV-2.[12,14−17] Multiplex RT-ddPCR has been evaluated on nasopharyngeal swab[16] and saliva samples,[15] resulting in an efficient quantitation of virus load. The comparison of the diagnostic sensitivity between RT-qPCR and RT-ddPCR for SARS-CoV-2 detection has revealed that implementation of RT-ddPCR eliminates false negative results[18,19] and enables accurate and sensitive quantification of low viral load of SARS-CoV-2 when compared to RT-qPCR.[20] Analytical and clinical validation of highly sensitive molecular assays is highly important for the reliable detection and quantification of SARS-COV-2 RNA transcripts, leading to a better management of infected patients,[21,22] confirmatory analysis of samples with high C_q values, and for viral detection in wastewater samples.[23]

We present here the development, analytical validation, and clinical evaluation of a novel one-step highly sensitive and specific five-plex one-step RT-ddPCR assay for the simultaneous absolute quantification of three different regions of the nucleoprotein (*N*) gene (N1, N2, N3) of SARS-CoV-2, a synthetic RNA of known concentration as an RNA exogenous control (RNA-EC), and Beta-2-Microglobulin (*B2M*) transcripts as an endogenous RNA internal control (RNA-IC).

MATERIALS AND METHODS

Development of One-Step Five-Plex RT-ddPCR. *In-Silico Design.* The development of one-step five-plex RT-ddPCR assay for the detection and quantification of SARS-COV-2 was based on an in-silico design of highly specific primers and probes targeting three different regions of the SARS-CoV2 *N* gene (N1, N2, N3), an RNA-EC, and an RNA-IC. Our in-silico design was based on specific amplification of SARS-COV2 VOCs and was focused on a gene area that is highly conserved and is not affected by different SARS-COV2 variants. The in-silico design was performed by using Primer Premier 5.0 software (Premier Biosoft, CA, USA). The specificity of primers and probes was initially tested by homology searches in the nucleotide database (NCBI, nucleotide BLAST) and for cross-reactivity among the five different transcripts. The specificity of primers and probes of N1, N2, and N3 gene transcripts was also checked against the alignment of 14 different coronaviruses (Table 1).

All hydrolysis probes were designed with a 6-carboxyfluorescein (FAM) or hexachlorofluorescein (HEX) fluorophore and ZEN/Iowa Black FQ quenchers for more efficient quenching (Integrated DNA Technologies, Inc., USA). The design of five-plex RT-ddPCR was based on probe-mixing and multiplexing by varying different ratios of FAM and HEX fluorescent dyes, resulting in five unique fluorescent signatures (Figure 1).

Five clearly separated clusters on a two-dimensional (2-D) scatter plot of the FAM and HEX amplitude were obtained by using the following ratios: N2 (100% FAM), N1 (70% FAM/30% HEX), EC (50% FAM/50% HEX), N3 (30% FAM/70% HEX), and IC (100% HEX). For the quantification of N1 and N3 transcripts, we did not use equal final concentrations of FAM and HEX Taqman probe, but primers and probes that had similar characteristics like GC content, length, melting temperature, and ΔG (Kcal/mol) number of nucleotides, thus minimizing the competitive nature of the reaction (Figure 1).

Table 1. In-silico Design for the Detection of Three Different Regions of the Viral Genome of SARS-COV-2: Alignment with 14 Different Coronaviruses

Coronovirus	accession number	N1	N2	N3
SARS coronavirus GZ02	AY390556.1	x	x	x
SARS coronavirus Sino1-11	AY485277	x	x	x
SARS coronavirus NS-1	AY508724	x	x	x
Bat coronavirus Cp/Yunnan2011	JX993988	x	x	x
BtRs-BetaCoV/GX2013	KJ473815	x	x	x
SARS-like coronavirus WIV16	KT444582	x	x	x
Bat SARS-like coronavirus isolate Rf4092	KY417145	x	x	x
Bat SARS-like coronavirus isolate Rs4231	KY417146	x	x	x
Bat SARS-like coronavirus isolate Rs4247	KY417148	x	x	x
Bat SARS-like coronavirus isolate Rs7327	KY417151	x	x	x
Bat coronavirus isolate Anlong-112	KY770859	x	x	x
Coronavirus BtRl-BetaCoV/SC2018	MK211374	x	x	x
Coronavirus BtRs-BetaCoV/YN2018C	MK211377	x	x	x
Bat coronavirus RaTG13	MN996532	x	x	x
severe acute respiratory syndrome coronavirus 2 isolate Wuhan-Hu-1	045512.2			

RNA-EC. A synthetic RNA oligo was in-silico designed to be used as an exogenous control to evaluate the performance of the whole analysis procedure. The designed RNA oligo is a 119 bp single-stranded synthetic RNA sequence that does not align to the human or SARS-COV genome. This synthesized RNA-EC is unique, contains unmodified RNA bases, and can be used in any RNA-specific molecular biology application.

Synthetic DNA Standards. We designed five synthetic DNA oligos that we used as standards for the evaluation of the analytical specificity of the five-plex RT-ddPCR assay. Each of these oligos contained the target sequences, including the primer and probe binding sites of: N1 (143 bp), N2 (132 bp), N3 (129 bp), EC (144 bp), and IC (130 bp). Each synthetic DNA oligo was diluted with Tris−EDTA (TE) buffer to obtain a stock solution with a concentration of 10 ng/μL.

One-Step RT-ddPCR. All details for one-step RT-ddPCR workflow and analytical and clinical validation are presented in Supporting Information file.

RESULTS AND DISCUSSION

Optimization of One-Step Five-Plex RT-ddPCR. *Annealing Temperature.* For the optimization of the annealing temperature, the five-plex RT-ddPCR was run across a thermal gradient of 53−63 °C. We selected 61 °C as the optimal annealing/extension temperature that achieves clear separation of all five clusters of droplets for each individual transcript.

Primers and Probes. We selected 0.75 μM as the optimal final concentration for the primers used in the assay. In order to evaluate the probe-mixing multiplexing, we checked two distinct approaches of different ratios of FAM and HEX probes. In the first approach, we examined the following ratios: N2 (100% FAM), N1 (70% FAM/30%HEX), EC (50% FAM/

https://doi.org/10.1021/acs.analchem.2c00868
Anal. Chem. XXXX, XXX, XXX−XXX

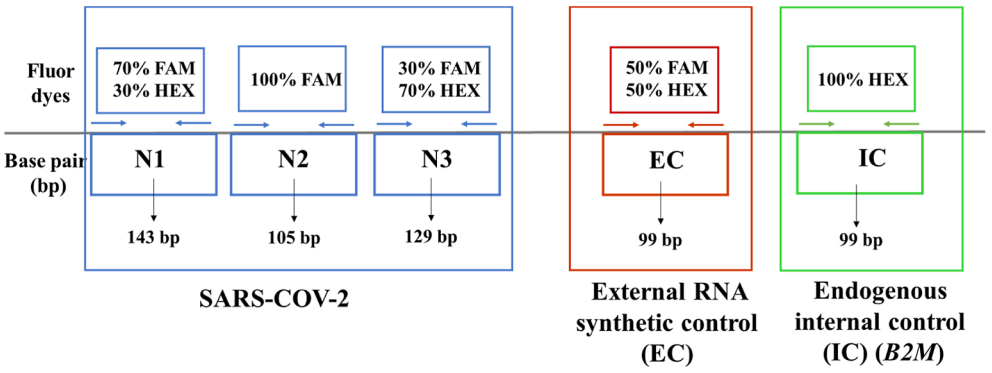

Figure 1. Targets of one-step five-plex RT-ddPCR SARS COV-2 assay.

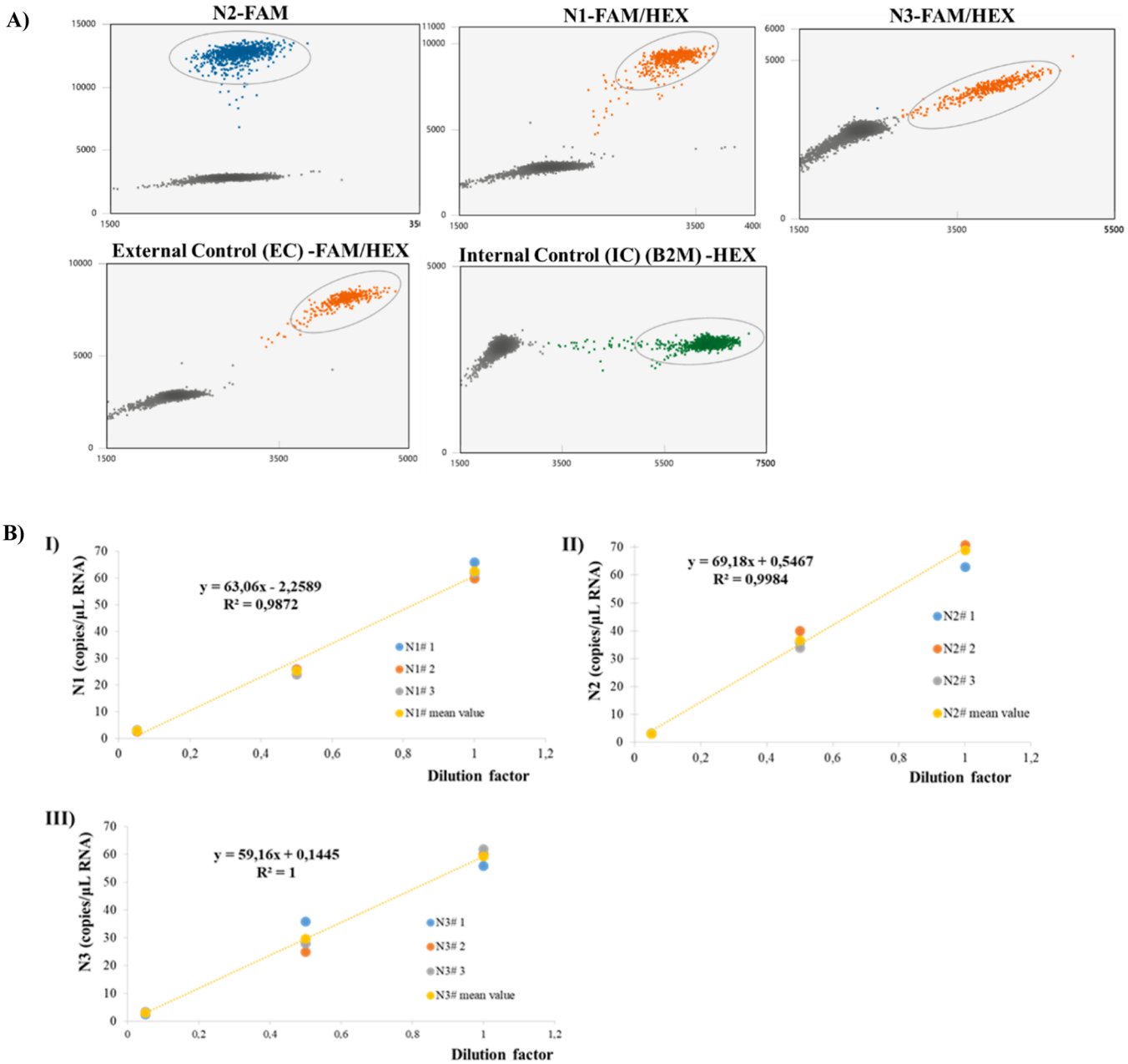

Figure 2. (A) Analytical specificity of the one-step five-plex RT-ddPCR depicted in five different 2-D plots corresponding to each gene target (N1, N2, N3, EC, and IC), (B) LDR of multiplex RT-ddPCR assay in serial 1:2 dilution series from 100 to 25 SARS-CoV-2 RNA copies/reaction for: (I) N1 gene transcript, (II) N2 gene transcript, and (III) N3 gene transcript.

https://doi.org/10.1021/acs.analchem.2c00868
Anal. Chem. XXXX, XXX, XXX−XXX

Table 2. One-Step Five-Plex RT-ddPCR Assay for SARS-COV-2: Intra-(n = 3) and Inter-Assay (n = 4) Precision

gene target	calibrators	copies/μL (SD)	CV %	mean copies per partition (λ^a) (SD)	CV %	partition number (n) (SD)	CV %
				Intra-Assay Precision (n = 3)			
N1	CAL1[a]	3.2 (0.40)	12	2.8×10^{-3} (0.31)	11	1.1×10^{4} (0.14)	13
	CAL2[a]	1.1 (0.17)	16	9.4×10^{-4} (1.6)	17	1.1×10^{4} (0.087)	8.1
	CAL3[a]	0.49 (0.061)	13	4.1×10^{-4} (0.54)	13	1.1×10^{4} (0.090)	8.5
N2	CAL1[a]	3.3 (0.31)	9.2	2.8×10^{-3} (0.34)	12	1.1×10^{4} (0.14)	13
	CAL2[a]	1.0 (0.15)	15	9.4×10^{-4} (1.4)	15	1.1×10^{4} (0.087)	8.1
	CAL3[a]	0.47 (0.051)	11	4.1×10^{-4} (0.59)	14	1.1×10^{4} (0.090)	8.5
N3	CAL1[a]	3.6 (0.35)	9.6	3.4×10^{-3} (0.48)	14	1.1×10^{4} (0.14)	13
	CAL2[a]	1.0 (0.060)	5.9	8.6×10^{-4} (0.48)	5.6	1.1×10^{4} (0.087)	8.1
	CAL3[a]	0.52 (0.11)	21	3.9×10^{-4} (0.96)	25	1.1×10^{4} (0.090)	8.5
RNA-EC	CAL1[a]	3.6 (0.20)	5.6	3.1×10^{-3} (0.15)	5.0	1.1×10^{4} (0.14)	13
	CAL2[a]	0.63 (0.090)	14	5.4×10^{-4} (0.79)	15	1.1×10^{4} (0.087)	8.1
	CAL3[a]	0.53 (0.11)	21	5.0×10^{-4} (0.87)	17	1.1×10^{4} (0.090)	8.5
RNA-IC	CAL1[a]	2.1 (0.17)	8.2	1.8×10^{-3} (0.17)	10	1.1×10^{4} (0.14)	13
	CAL2[a]	0.41(0.087)	21	3.5×10^{-4} (0.74)	21	1.1×10^{4} (0.087)	8.1
	CAL3[a]	0.22 (0.023)	10	1.9×10^{-4} (0.17)	8.7	1.1×10^{4} (0.090)	8.5
				Inter-Assay Precision (n = 4)			
N1	CAL4[b]	1.0×10^{1} (0.14)	14	8.6×10^{-3} (1.2)	14	1.4×10^{4} (0.29)	21
	CAL5[b]	5.7 (1.0)	18	4.4×10^{-3} (0.89)	20	1.2×10^{4} (0.12)	9.8
	CAL6[b]	2.2 (0.33)	15	1.9×10^{-3} (0.26)	14	1.2×10^{4} (0.12)	10
N2	CAL4[b]	1.4×10^{1} (0.098)	7.0	1.2×10^{-2} (0.080)	6.7	1.4×10^{4} (0.29)	21
	CAL5[b]	6.3 (0.56)	9.0	5.0×10^{-3} (0.51)	10	1.2×10^{4} (0.12)	9.8
	CAL6[b]	2.4 (0.30)	13	2.1×10^{-3} (0.25)	12	1.2×10^{4} (0.12)	10
N3	CAL4[b]	1.4×10^{1} (0.19)	14	1.2×10^{-2} (0.15)	13	1.4×10^{4} (0.29)	21
	CAL5[b]	7.4 (0.43)	5.8	6.2×10^{-3} (0.37)	6.0	1.2×10^{4} (0.12)	9.8
	CAL6[b]	3.2 (0.59)	18	2.7×10^{-3} (0.49)	19	1.2×10^{4} (0.12)	10
RNA-EC	CAL4[b]	2.8×10^{1} (0.37)	13	2.4×10^{-2} (0.32)	13	1.4×10^{4} (0.29)	21
	CAL5[b]	1.4×10^{1} (0.11)	8.1	1.2×10^{-2} (0.12)	10	1.2×10^{4} (0.12)	9.8
	CAL6[b]	6.4 (0.50)	7.9	5.4×10^{-3} (0.43)	7.8	1.2×10^{4} (0.12)	10
RNA-IC	CAL4[b]	2.2×10^{1} (0.25)	12	1.8×10^{-2} (0.22)	12	1.4×10^{4} (0.29)	21
	CAL5[b]	1.1×10^{1} (0.062)	5.8	8.8×10^{-3} (1.1)	13	1.2×10^{4} (0.12)	9.8
	CAL6[b]	3.5 (0.54)	15	3.0×10^{-3} (0.47)	16	1.2×10^{4} (0.12)	10

[a]$\lambda = -\ln(1 - k/n)$, k: number of positive partitions and n: number of partitions, (a): mix of AcroMetrix Coronavirus 2019 (COVID-19) RNA Control, and EC and RNA derived from the MCF-7 cell line, (b): mix of RNA derived from a SARS-COV-2(+) clinical sample, and the EC and RNA from the MCF-7 cell line.

50% HEX), N3 (30% FAM/70% HEX), and IC (100% HEX), while in our second approach, we performed the following: N2 (100% FAM), N1 (60% FAM/40%HEX), EC (50% FAM/50% HEX), N3 (40% FAM/60% HEX), and IC clusters had equal distances among them in a 2-D plot, resulting in better separation (results not shown).

Analytical Validation. Analytical validation of the developed assay was performed according to MIQE guidelines for quantitative digital PCR experiments.[24] We used synthetic and/or human DNA and RNA calibrators to estimate limit of blank (LOB), limit of detection (LOD), limit of quantification (LOQ), intra- and inter-assay repeatability, analytical recovery, linear dynamic range (LDR), and analytical sensitivity and specificity. The availability of specific traceability in validated controls is critical for analytical method development and validation.[25,26] Recently, an RNA reference material of SARS-CoV-2 was produced and characterized using ddPCR as a quality control assessment of molecular COVID-19 tests.[27]

Analytical Specificity. For the evaluation of the analytical specificity of the assay, five DNA synthetic standard solutions, each specific for each target transcript, were prepared to a final concentration of 100 copies/μL. The analytical specificity of the assay was then tested by using as sample only 1 μL of each individual DNA synthetic standard in the absence of all others, representing one specific target transcript in five individual reactions of the five-plex RT-qPCR. Then, one-step five-plex RT-ddPCR was performed in the presence of all primers and probes for all transcripts. According to our results, the analytical specificity of the assay is excellent; as can be seen in Figure 2A in a 2-D plot, in these five individual RT-ddPCR reactions, only one droplet cluster is obtained corresponding to the specific gene target added in each case.

Linear Dynamic Range. The LDR of each primer/probe set of N gene was evaluated across serial 1:2 dilutions from 100 to 25 SARS-CoV-2 RNA copies/reaction through a linear regression plot representing the absolute number of copies/reaction (Y-axis) in relation to the dilution factor. All reactions were performed in triplicate. The correlation coefficient for all transcripts was higher than 0.98, indicating a precise linear relationship (Figure 2B). The linearity of the developed five-plex RT-ddPCR assay was very satisfactory over a broad concentration range for N1, N2, and N3 gene transcripts (Figure 2B).

Analytical Sensitivity. LOB, LOD, and LOQ of the multiplex RT-ddPCR assay were defined as previously described.[28] For this purpose, RNA samples derived from 15 healthy donors were used to determine LOB; all were negative, while RNA-IC was positive. For LOD estimation, we used a

https://doi.org/10.1021/acs.analchem.2c00868
Anal. Chem. XXXX, XXX, XXX−XXX

Table 3. Analytical Recovery of the Developed One-Step Five-Plex RT-ddPCR SARS-CoV-2 Assay Using Three Different Calibrators of Known Concentrations in Triplicate

calibrators	added copies/reaction	found N1 copies ± SD (n = 3)	found N2 copies ± SD (n = 3)	found N3 copies ± SD (n = 3)	found N1, N2, N3, mean value ± SD (n = 9)	recovery (%) (range, CV %)
CAL1	70	65 ± 0.40	67 ± 0.31	72 ± 0.35	68 ± 3.8	96.8 (92.4−103, 5.6%)
CAL2	25	22 ± 0.17	21 ± 0.15	20 ± 0.060	21 ± 0.86	84.1 (81.6−88.0, 4.1%)
CAL3	12.5	9.7 ± 0.061	9.5 ± 0.051	10 ± 0.11	10 ± 0.48	78.9 (75.7−83.2, 4.9%)

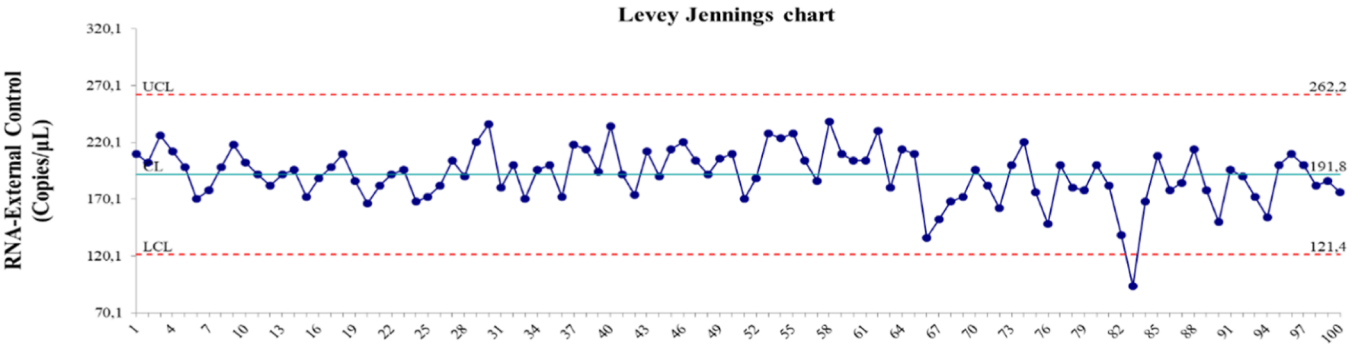

Figure 3. Levey−Jennings graph of all measurements for RNA-EC (n = 100).

commercially available RNA control (AcroMetrix COVID-19 RNA Control) of known concentration at three different concentrations (CAL1:70 copies/reaction, CAL2:25 copies/reaction, and CAL3:12.5 copies/reaction) run in triplicate (Table 2).

The LOD for each of the three distinct genomic areas of the SARS-CoV-2 N gene (N1, N2, N3) was 0.13 copies/μL of ddPCR reaction (that means 2.5 copies/μL of RNA sample input), and its estimation was based on the SD values derived from CAL3 measurements (Table 2).

LOQ was set as the lowest positive droplet count that had a CV ≤ 25%. As shown in Table 2, the number of CAL3 transcripts, which correspond to the lowest positive droplet count that had a CV ≤ 25%, was 0.5 copies/μL (that means 10 copies/μL of RNA sample input) (Table 2).

Intra- and Inter-Assay Repeatability. To evaluate the intra- and inter-assay repeatability of the developed assay, the concentration of each gene transcript, the mean copies per partition (λ), and the partition number (n) of each analytical run were calculated according to the digital MIQE guidelines.[24] Intra-assay repeatability of the five-plex RT-ddPCR assay was evaluated by analyzing within the same RT-ddPCR run three different concentrations of a commercially available calibrator, with known SARS-CoV2 concentration (CAL1, CAL2, and CAL3) in triplicate (Table 2). CV % ranged from 12 to 16% for N1, 9.2 to 15% for N2, 5.9 to 21% for N3, 5.6 to 21% for RNA-EC, and 8.2 to 21% for RNA-IC. Reproducibility or inter-assay variance was evaluated by analyzing three samples prepared by mixing in equal copy numbers: RNA derived from a SARS-CoV-2 positive clinical sample and the RNA-EC and RNA-IC (RNA derived from the MCF-7 cell line) with (CAL4, CAL5, CAL6) in four separate RT-ddPCR runs performed on four different days (Table 2). CV % in this case ranged from 14 to 18% for N1, 7.0 to 13% for N2, 5.8 to 18% for N3, 7.9 to 13% for RNA-EC, and 5.8 to 15% for RNA-IC.

Analytical Recovery. The analytical recovery of the developed five-plex one-step RT-ddPCR for the quantification of N1, N2, and N3 transcripts was determined using a commercially available RNA control (AcroMetrix COVID-19 RNA Control) of known concentration at three different concentrations (CAL1:70 copies/reaction, CAL2:25 copies/reaction, and CAL3:12.5 copies/reaction). These three samples were quantified by the developed RT-ddPCR in three individual reactions in triplicate (Table 3). Analytical recovery (%) was calculated by dividing the copy number of each N gene transcript as found by RT-ddPCR by the known added copy number in each case and multiplying by 100. For CAL1, analytical recovery ranged from 92.4 to 103%; for CAL2 from 81.6 to 88.0%; and for CAL3 from 75.7 to 83.2%, with CV % across reaction replicates ranging from 4.1% to 5.6% (Table 3).

Quality Control. *RNA-EC.* In each reaction, 4000 copies (200 copies/μL) of RNA-EC were spiked to verify high performance of droplet generation and one-step five-plex RT-ddPCR reaction. 100 copies/μL out of the 200 copies/μL were detected in the FAM channel, while the remaining 100 copies/μL were detected in the HEX channel. The mean recovery rate of 100 measurements in each fluorescence amplitude was 97.01 ± 9.0, and the CV % was 9.3% (Supporting Information file). The distribution of the absolute number of copies of RNA-EC among all measurements is depicted in a representative Levey−Jennings graph (Figure 3).

It is known that, universal RNA standards provide information on the performance of different molecular platforms and methodologies.[29] Thus, we de novo designed for the first time an external, stable, and unique synthetic RNA control that has no homology to the human or coronavirus genome. The spiking of RNA-EC in each reaction ensured the good performance of the droplet generator, RT-ddPCR reagents, thermal cycler, and QX200 Droplet Reader. The high recovery rate of RNA-EC in all samples tested ensured the reproducibility of all steps of the developed protocol.

RNA-IC. Quantification of the RNA-IC (*B2M* transcripts) in each clinical sample verifies the accurate sampling of columnar epithelial cells, and that all experimental steps of the assay

https://doi.org/10.1021/acs.analchem.2c00868
Anal. Chem. XXXX, XXX, XXX−XXX

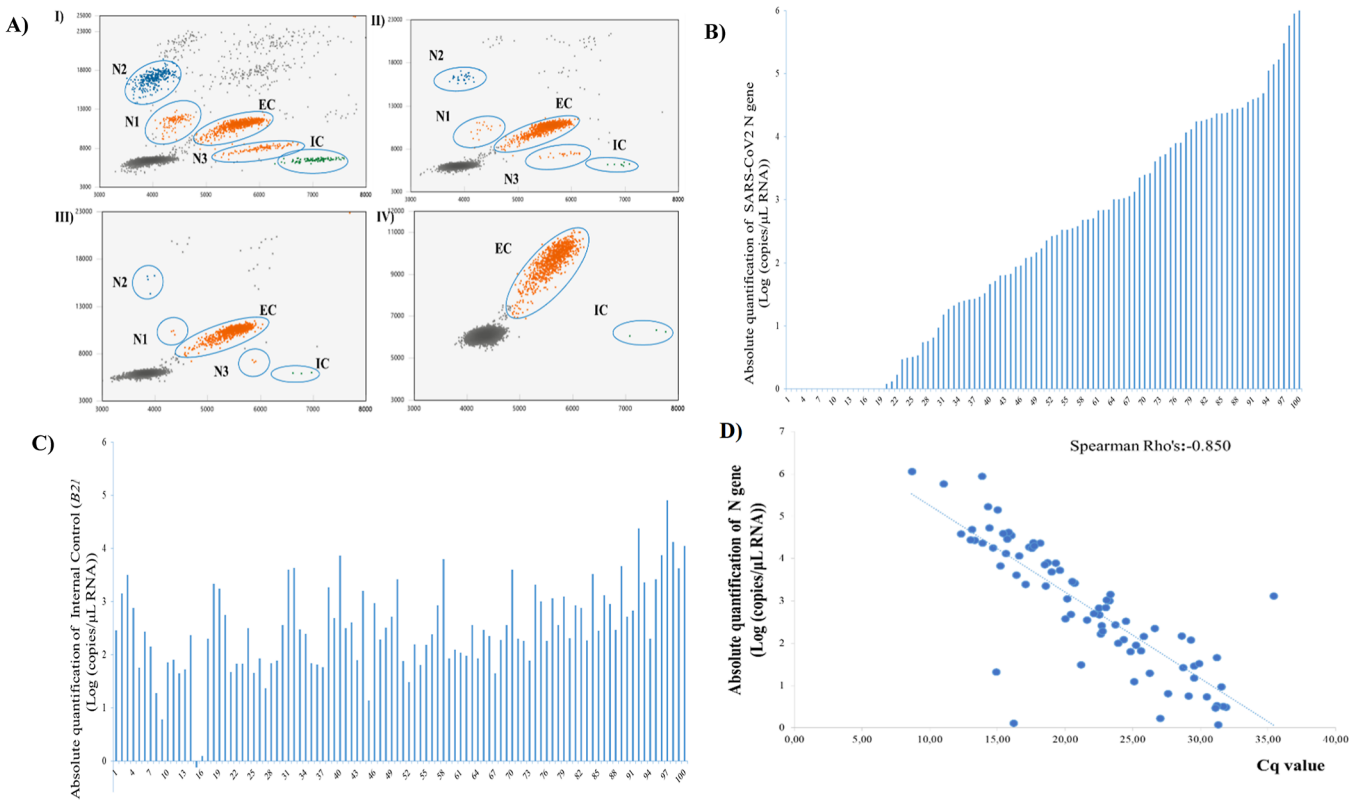

Figure 4. (A) 2-D plots of five-plex RT-ddPCR assay of (a) clinical sample with a high viral load, (b) clinical sample with a low viral load, (c) clinical sample with an ultra-low viral load, and (d) negative sample, (B) absolute number of viral RNA copies of all clinical samples analyzed in the ascending order, (C) corresponding absolute number of IC (B2M) copies, (D) Spearman's correlation between C_t values and absolute number of copies of SARS-COV-2 in identical RNA samples (n = 80).

worked well. Moreover, the detection of *B2M* transcripts in each sample confirms the absence of false negative results.

The inclusion of external RNA-EC control in all RNA samples in parallel with the simultaneous amplification and detection of *B2M* as an RNA-IC is highly important for the immediate exclusion of potential false negative results due to low sample quality or pre-analytical errors.

Quantification of SARS-CoV-2-Transcripts in Nasopharyngeal and/or Oropharyngeal Swabs. We applied the developed one-step five-plex RT-ddPCR for the quantification of SARS-CoV-2-transcripts in 100 RNA samples, collected from nasopharyngeal and/or oropharyngeal swabs, by using 5 μL of RNA in each RT-ddPCR reaction. All these samples were collected within one year, and RNAs were kept at −80 C till the analysis by RT-ddPCR. In all samples, the same amount of RNA-EC was added. According to our RT-ddPCR results, 19/100 (19.0%) were found negative, while 81/100 (81.0%) were found positive for SARS-CoV-2 transcripts. The mean number of copies per μL of RNA of each transcript was 3.5 × 104 for N1 transcript (range: 0.64−9.7 × 105), 3.8 × 104 for N2 transcript (range: 1.28−1.1 × 106), and 3.8 × 104 for N3 transcript (range: 1.92−1.4 × 106). We then compared our quantitative results for these three transcripts of the *N* gene (N1, N2, N3) by performing the Kruskal−Wallis test and concluded that the distribution of the absolute number of copies of *N* gene is the same (p = 0.950) (Supporting Information file).

We chose to amplify three different regions of the nucleocapsid (*N*) gene for the quantification of SARS-CoV-2 in clinical samples. The nucleocapsid protein is the main structural protein of SARS-CoV-2 and plays an important role in the viral life cycle while is abundantly expressed during viral infection.[30] A recent study has shown that the selection of the N gene instead of the *ORF-1b* region provides higher sensitivity in detecting positive clinical specimens.[1] Given the fact that there is an extended alignment between different coronaviruses in specific genome regions,[31] we performed a detailed in silico design to provide specific detection of SARS-CoV-2. Moreover, the selection of three regions instead of one increases the probability of detection of SARS-CoV-2, especially in samples with a low viral load. Apart from that, the examination of multiple gene areas excludes false negative results due to genetic diversity.[32]

As shown in Figure 3, the concentration of the added RNA-EC found by RT-ddPCR in each sample was almost the same regardless of the viral load of the clinical specimens. In Figure 4A, four representative 2-D plots are shown: (a) a clinical sample with a high viral load, (b) a clinical sample with a low viral load, (c) a clinical sample with an ultra-low viral load, and (d) a negative sample. Copies of RNA-IC were quantified in all clinical samples. The mean number of copies per μL of RNA was 2.1 × 10^3(range: 0.76−8.0 × 10^5). In Figure 4B, the mean absolute number of viral RNA copies of each clinical sample is shown in the ascending order; in Figure 4C, the absolute number of RNA-IC transcripts of the corresponding samples is shown.

Similar levels of copies of SARS-COV-2 were found in all three regions, indicating equal efficiencies off all three different single reactions included in the same multiplex setting. The viral load of clinical specimens ranged from very low to very

https://doi.org/10.1021/acs.analchem.2c00868
Anal. Chem. XXXX, XXX, XXX−XXX

high number of copies, indicating a particular heterogeneity of virus infection. These differences in viral load levels are associated to the duration of the disease and activation of interferon pathway genes.[33] Understanding patient heterogeneity could help clinicians to decide on time which patients need more aggressive treatment and which patients could benefit by the administration of specific therapies.[34]

Quantification of *B2M* transcripts, used as an RNA-IC in all tested clinical samples, revealed that differences in viral load levels are not only due to patient heterogeneity but also differences in sampling recoveries, as columnar epithelial cells express *B2M*. Biological sampling is a very important parameter in the collection of nasopharyngeal specimens since suboptimal sampling could contribute to false negative results.[35] In the developed assay, the parallel amplification of *B2M* in all samples as an RNA-IC and absolute quantification using ddPCR technology provide accurate and sensitive quantification of virus load in clinical specimens, even in cases with limited sample processing.[36]

Direct Comparison of the Developed One-Step Five-Plex RT-ddPCR with a Commercially Available CE-IVD RT-qPCR Assay. The developed one-step five-plex RT-ddPCR assay was directly compared with a commercially available CE-IVD RT-qPCR assay (VIASURE SARS-CoV-2 kit,CerTest BIOTECH Inc). For this reason, the same 100 RNA samples, collected by nasopharyngeal and/or oropharyngeal swabs, were analyzed by both methods. According to the RT-qPCR results, 20/100 (20.0%) were found negative, while 80/100 (80.0%) were found positive for SARS-COV-2. The C_q values obtained by RT-qPCR for these 80 positive samples were highly correlated with the absolute number of copies obtained by RT-ddPCR using Spearman's rank correlation coefficient (Figure 4D). More specifically, there was a strong negative correlation (Spearman's correlation coefficient = −0.850; $p < 0.001$) between C_q values and absolute number of copies; lower C_q values were highly correlated with a high number of copies as found by RT-ddPCR, while higher C_q values were correlated with a low number of copies. However, there was one sample with a low viral load that was found positive using one-step five-plex RT-ddPCR but was negative with RT-qPCR. This is in agreement with other studies showing that ddPCR has better performance for the quantification of rare sequence variants when compared to RT-qPCR,[37,38] even in the presence of a high background.[39]

The main advantage of the developed one-step five-plex RT-ddPCR assay, in comparison to other multiplex RT-ddPCR as says,[14−17] is the inclusion of an RNA-EC and an RNA-IC and their simultaneous amplification with three transcripts of SARS-COV-2. Recently, a six-plex RT-ddPCR assay for the detection of two different genes of SARS-COV-2 genome and an RNA-dependent RNA polymerase (RdRp) was reported.[15] However, no control was used. De Kock et al. developed a multiplex RT-ddPCR assay for the detection of SARS-COV-2 using two different ICs but no EC. Although IC is essential for evaluating successful sample collection, the use of an EC is highly important for quality control assessment of RT-ddPCR assays since it is the most complete control type for reagent validation[40] and for testing the performance in each discrete ddPCR reaction.

CONCLUSIONS

In conclusion, we report the development, analytical validation, and clinical performance of a novel one-step five-plex RT-ddPCR assay for the absolute and simultaneous quantification of three different regions (N1, N2, N3) of SARS-COV-2 nucleocapsid gene, an RNA-EC, and an RNA-IC. The simultaneous absolute quantification of the RNA-EC and RNA-IC provides quality control assessment that is highly important and critical for the standardization and reliability of the results. The direct comparison of the developed one-step five-plex RT-ddPCR assay with a commercially available CE-IVD RT-qPCR kit revealed a very high concordance and a higher sensitivity in SARS-COV-2 detection compared to RT-qPCR. The developed assay can be directly applied for the reliable detection and quantification of SARS-COV-2 RNA transcripts in clinical and wastewater samples.

ASSOCIATED CONTENT

Supporting Information

The Supporting Information is available free of charge at https://pubs.acs.org/doi/10.1021/acs.analchem.2c00868.

Materials and Methods, one-step RT-ddPCR, recovery (%) and RSD (%) obtained from one-step RT-ddPCR analysis of clinical samples (n = 100) spiked with 4000 copies (200 copies/μL) of RNA-external control; and Kruskal−Wallis test for the comparison of the distribution of N1, N2, and N3 absolute number of copies among 81 clinical samples (PDF)

AUTHOR INFORMATION

Corresponding Authors

Areti Strati − *Lab of Analytical Chemistry, Department of Chemistry, National and Kapodistrian University of Athens, 15771 Athens, Greece;* orcid.org/0000-0001-9644-5538; Email: astrati@chem.uoa.gr

Evi S. Lianidou − *Lab of Analytical Chemistry, Department of Chemistry, National and Kapodistrian University of Athens, 15771 Athens, Greece;* orcid.org/0000-0002-7796-5914; Email: lianidou@chem.uoa.gr

Authors

Martha Zavridou − *Lab of Analytical Chemistry, Department of Chemistry, National and Kapodistrian University of Athens, 15771 Athens, Greece;* Present Address: M.Z.—Department of Genitourinary Medical Oncology, The University of Texas MD Anderson Cancer Center, Houston, TX, 77030, USA

Dimitrios Paraskevis − *Department of Hygiene, Epidemiology and Medical Statistics, Medical School, National and Kapodistrian University of Athens, 11527 Athens, Greece*

Gkikas Magiorkinis − *Department of Hygiene, Epidemiology and Medical Statistics, Medical School, National and Kapodistrian University of Athens, 11527 Athens, Greece*

Spyros Sapounas − *National Public Health Organization, 15123 Athens, Greece*

Pagona Lagiou − *Department of Hygiene, Epidemiology and Medical Statistics, Medical School, National and Kapodistrian University of Athens, 11527 Athens, Greece*

Nikolaos S. Thomaidis − *Lab of Analytical Chemistry, Department of Chemistry, National and Kapodistrian University of Athens, 15771 Athens, Greece;* orcid.org/0000-0002-4624-4735

Complete contact information is available at: https://pubs.acs.org/10.1021/acs.analchem.2c00868

Author Contributions

The manuscript was written through contributions of all authors. A.S. conceived the experiments, analyzed the results, supervised the project, and wrote and edited the manuscript draft; M.Z. conducted some experiments under the supervision of A.S.; D.P., G.M., S.S., and M.L. provided clinical samples; N.T. provided some resources: E.L. supervised the project, edited the manuscript draft, and was responsible for funding acquisition.

Notes

The authors declare no competing financial interest.

■ ACKNOWLEDGMENTS

The authors would like to thank National and Kapodistrian University of Athens Special Account for Research Grants (NKUA-SARG) for financial support. PL and GM gratefully acknowledge donations from SYN-ENOSIS, the Greek Shipowners' Social Welfare Company. This funding source had no role in the design of this study and did not have any role during its execution, analyses, interpretation of the data, or decision to submit the results.

■ LIST OF ABBREVIATIONS

NAATs	nucleic acid amplification tests
C_q	quantification cycle
RNA-EC	RNA exogenous control
RNA-IC	RNA internal control
B2M	beta-2-microglobulin
N	nucleoprotein
FAM	6-carboxyfluorescein
HEX	hexachlorofluorescein
TE	Tris−EDTA
DTT	dithiothreitol
LOD	limit of detection
LOQ	limit of quantification
LDR	linear dynamic range
RdRp	RNA-dependent RNA polymerase

■ REFERENCES

(1) Chu, D. K. W.; Pan, Y.; Cheng, S. M. S.; Hui, K. P. Y.; Krishnan, P.; Liu, Y.; Ng, D. Y. M.; Wan, C. K. C.; Yang, P.; Wang, Q.; et al. *Clin. Chem.* **2020**, *66*, 549−555.
(2) Kevadiya, B. D.; Machhi, J.; Herskovitz, J.; Oleynikov, M. D.; Blomberg, W. R.; Bajwa, N.; Soni, D.; Das, S.; Hasan, M.; Patel, M.; et al. *Nat. Mater.* **2021**, *20*, 593−605.
(3) Diagnostic testing and screening for SARS-CoV-2 https://www.ecdc.europa.eu/en/covid-19/latest-evidence/diagnostic-testing (accessed on Oct 4, 2021).
(4) CDC Diagnostic Tests for COVID-19 | CDC https://www.cdc.gov/coronavirus/2019-ncov/lab/testing.html (accessed on Oct 4, 2021).
(5) Test for Past Infection|CDC https://www.cdc.gov/coronavirus/2019-ncov/testing/serology-overview.html (accessed on Oct 4, 2021).
(6) Gill, D.; Ponsford, M. J. *BMJ* **2020**, *371*, m4288.
(7) Interim Guidelines for COVID-19 Antibody Testing | CDC https://www.cdc.gov/coronavirus/2019-ncov/lab/resources/antibody-tests-guidelines.html (accessed on Oct 4, 2021).
(8) Dinnes, J.; Sharma, J. J.; Berhane, A.; van Wyk, S.; Nyaaba, C.; Domen, S.; Taylor, D.; Cunningham, Y.; Davenport, J.; Dittrich, S.; et al. *Cochrane Database Syst. Rev.* **2022**, *7*, CD013705.
(9) Doykov, I.; Hällqvist, J.; Gilmour, K. C.; Grandjean, L.; Mills, K.; Heywood, W. E. *F1000Research* **2020**, *9*, 1349.
(10) Zapor, M. *Viruses* **2020**, *12*, 1384.
(11) Rao, S. N.; Manissero, D.; Steele, V. R.; Pareja, J. *Infect. Dis. Ther.* **2020**, *9*, 573−586.
(12) Tan, C.; Fan, D.; Wang, N.; Wang, F.; Wang, B.; Zhu, L.; Guo, Y. *View* **2021**, *2*, 20200082.
(13) Whale, A. S.; Huggett, J. F.; Tzonev, S. *Biomol. Detect. Quantif.* **2016**, *10*, 15−23.
(14) de Kock, R.; Baselmans, M.; Scharnhorst, V.; Deiman, B. *Eur. J. Clin. Microbiol. Infect. Dis.* **2021**, *40*, 807−813.
(15) Cassinari, K.; Alessandri-Gradt, E.; Chambon, P.; Charbonnier, F.; Gracias, S.; Beaussire, L.; Alexandre, K.; Sarafan-Vasseur, N.; Houdayer, C.; Etienne, M.; et al. *Clin. Chem.* **2021**, *67*, 736−741.
(16) Deiana, M.; Mori, A.; Piubelli, C.; Scarso, S.; Favarato, M.; Pomari, E. *Sci. Rep.* **2020**, *10*, 18764.
(17) Telwatte, S.; Martin, H. A.; Marczak, R.; Fozouni, P.; Vallejo-Gracia, A.; Kumar, G. R.; Murray, V.; Lee, S.; Ott, M.; Wong, J. K.; et al. *Methods* **2022**, *201*, 15.
(18) Xu, J.; Kirtek, T.; Xu, Y.; Zheng, H.; Yao, H.; Ostman, E.; Oliver, D.; Malter, J. S.; Gagan, J. R.; SoRelle, J. A. *Am. J. Clin. Pathol.* **2021**, *155*, 815−822.
(19) Alteri, C.; Cento, V.; Antonello, M.; Colagrossi, L.; Merli, M.; Ughi, N.; Renica, S.; Matarazzo, E.; Di Ruscio, F.; Tartaglione, L.; et al. *PLoS One* **2020**, *15*, No. e0236311.
(20) Poggio, P.; Songia, P.; Vavassori, C.; Ricci, V.; Banfi, C.; Barbieri, S. S.; Garoffolo, G.; Myasoedova, V. A.; Piacentini, L.; Raucci, A.; et al. *Sci. Rep.* **2021**, *11*, 4310.
(21) Kim, K. B.; Choi, H.; Lee, G. D.; Lee, J.; Lee, S.; Kim, Y.; Cho, S. Y.; Lee, D. G.; Kim, M. *Mol. Diagn. Ther.* **2021**, *25*, 617−628.
(22) Wang, D.; Wang, Z.; Gao, Y.; Wu, X.; Dong, L.; Dai, X.; Gao, Y. *J. Virol. Methods* **2021**, *298*, 114285.
(23) Galani, A.; Aalizadeh, R.; Kostakis, M.; Markou, A.; Alygizakis, N.; Lytras, T.; Adamopoulos, P. G.; Peccia, J.; Thompson, D. C.; Kontou, A.; et al. *Sci. Total Environ.* **2022**, *804*, 150151.
(24) Whale, A. S.; De Spiegelaere, W.; Trypsteen, W.; Nour, A. A.; Bae, Y.-K.; Benes, V.; Burke, D.; Cleveland, M.; Corbisier, P.; Devonshire, A. S.; et al. *Clin. Chem.* **2020**, *66*, 1012−1029.
(25) Dong, L.; Wang, S.; Fu, B.; Wang, J. *Sci. Rep.* **2018**, *8*, 9650.
(26) Deprez, L.; Corbisier, P.; Kortekaas, A. M.; Mazoua, S.; Beaz Hidalgo, R.; Trapmann, S.; Emons, H. *Biomol. Detect. Quantif.* **2016**, *9*, 29−39.
(27) Akyurek, S.; Demirci, S. N. S.; Bayrak, Z.; Isleyen, A.; Akgoz, M. *Anal. Bioanal. Chem.* **2021**, *413*, 3411−3419.
(28) Strati, A.; Zavridou, M.; Economopoulou, P.; Gkolfinopoulos, S.; Psyrri, A.; Lianidou, E. *Clin. Chem.* **2021**, *67*, 642−652.
(29) Devonshire, A. S.; Elaswarapu, R.; Foy, C. A. *BMC Genom.* **2011**, *12*, 1−10.
(30) McBride, R.; van Zyl, M.; Fielding, B. C. *Viruses* **2014**, *6*, 2991.
(31) Chen, Z.; Boon, S. S.; Wang, M. H.; Chan, R. W. Y.; Chan, P. K. S. *J. Virol. Methods* **2021**, *289*, 114032.
(32) Bahreini, F.; Najafi, R.; Amini, R.; Khazaei, S.; Bashirian, S. *Int. J. Matern. Child Heal. AIDS* **2020**, *9*, 408−410.
(33) Desai, N.; Neyaz, A.; Szabolcs, A.; Shih, A. R.; Chen, J. H.; Thapar, V.; Nieman, L. T.; Solovyov, A.; Mehta, A.; Lieb, D. J.; et al. *Nat. Commun.* **2020**, *11*, 6319.
(34) Rheumatology, T. L. *Lancet Rheumatol* **2020**, *2*, No. e577.
(35) Kinloch, N. N.; Ritchie, G.; Brumme, C. J.; Dong, W.; Dong, W.; Lawson, T.; Jones, R. B.; Montaner, J. S. G.; Leung, V.; Romney, M. G.; et al. *medRxiv* **2020**, *222*, 899−902.
(36) Vasudevan, H. N.; Xu, P.; Servellita, V.; Miller, S.; Liu, L.; Gopez, A.; Chiu, C. Y.; Abate, A. R. *Sci. Rep.* **2021**, *11*, 780.
(37) Liu, X.; Feng, J.; Zhang, Q.; Guo, D.; Zhang, L.; Suo, T.; Hu, W.; Guo, M.; Wang, X.; Huang, Z.; et al. *Emerg. Microb. Infect.* **2020**, *9*, 1175−1179.
(38) Suo, T.; Liu, X.; Feng, J.; Guo, M.; Hu, W.; Guo, D.; Ullah, H.; Yang, Y.; Zhang, Q.; Wang, X.; et al. *Emerg. Microb. Infect.* **2020**, *9*, 1259−1268.
(39) Taylor, S. C.; Laperriere, G.; Germain, H. *Sci. Rep.* **2017**, *7*, 2409.

https://doi.org/10.1021/acs.analchem.2c00868
Anal. Chem. XXXX, XXX, XXX−XXX

(40) Lim, L. P.; Lau, N. C.; Garrett-Engele, P.; Grimson, A.; Schelter, J. M.; Castle, J.; Bartel, D. P.; Linsley, P. S.; Johnson, J. M. *Nature* **2005**, *433*, 769−773.

https://doi.org/10.1021/acs.analchem.2c00868
Anal. Chem. XXXX, XXX, XXX−XXX